Desalination 474 (2020) 114180

Contents lists available at ScienceDirect

Desalination

journal homepage: www.elsevier.com/locate/desal

PRODUCT CHARACTERISTICS IN SIMULTANEOUS CRYSTALLIZATION OF NaCl AND $CaSO_4$ FROM AQUEOUS SOLUTION WITH SEEDING

G.P. Zago[a], F.M. Penha[a,b], M.M. Seckler[a,*]

[a] University of São Paulo, Polytechnic School, Department of Chemical Engineering, São Paulo, SP, Brazil
[b] Delft University of Technology, 3ME Faculty, Process & Energy Department, Intensified Reaction & Separation Systems Group, P&E Laboratory, Leeghwaterstraat 39, 2628 CB Delft, The Netherlands

ARTICLE INFO

Keywords:
Water reuse
Simultaneous crystallization
Batch evaporative crystallization
Sodium chloride
Calcium sulphate

ABSTRACT

Zero liquid discharge strategies for industrial wastewater treatment have become prominent in recent years. When evaporative simultaneous crystallization is applied, knowledge about the particle crystallization mechanisms and morphology are important to ease solids downstream handling and for recovery of their valuable components. In this work, batch simultaneous crystallization of sodium chloride (NaCl) and calcium sulphate hemihydrate ($CaSO_4.0.5H_2O$) from aqueous solution was studied. It was found that $CaSO_4.0.5H_2O$ is not an effective substrate for NaCl heterogeneous nucleation, but agglomerates with NaCl particles instead. $CaSO_4.0.5H_2O$ particles on the surface of NaCl crystals sterically hamper agglomeration of NaCl particles with each other and, for a sufficiently high $CaSO_4.0.5H_2O$ seed load, cover the NaCl crystals so that NaCl supersaturation rises, inducing NaCl primary nucleation. Simultaneous crystallization of $CaSO_4.0.5H_2O$ and NaCl yields a satisfactory product for downstream handling even for high $CaSO_4.0.5H_2O$ content in the crystallizer. However, seeding with $CaSO_4.0.5H_2O$ is not recommended as it reduces the mean size and increases product size dispersion. NaCl seeding may be considered if it is desirable to separate $CaSO_4.0.5H_2O$ from NaCl downstream the crystallizer by size classification, as it favors $CaSO_4.0.5H_2O$ to build up in product sizes of 200 μm and below.

1. Introduction

The development of alternatives to overcome water scarcity in industry has been drawing attention over the last decades. In the past, wastewater treatment aiming at the protection of water bodies from industrial discharges was considered sufficient. With time, the concept of treatment aiming at water reuse has become dominant, as it both prevents brine disposal to the environment and accommodates water needs. Among the latest efforts for industrial wastewater management, the so-called zero liquid discharge strategies have become prominent [1–3], in which brine disposal is avoided and only a small amount of solid waste is generated. In principle, further treatment of the solids would enable the economic recovery of at least some of their components, further reducing the environmental impact of water use in industry.

Crystallization alternatives for wastewater treatment aiming at zero liquid discharge are currently either available or in development, the main options being evaporative crystallization, membrane assisted crystallization and eutectic freeze crystallization [4–8]. Regardless of the crystallization option, water is removed either as a vapor or as ice, whereas the solids crystallize from an aqueous solution. Crystallization of just one solute from a multicomponent solution is rather well known, but simultaneous crystallization of two or more solids is much less studied. Despite its potential, simultaneous crystallization is still avoided in industrial crystallizers, as the product from such operation often ends up in unexpected particle characteristics that might hinder downstream operations. Besides, the particulate product from simultaneous crystallization is comprised of single particles of each compound and mixed composition polycrystalline particles [9,10]. Mixed composition particles are difficult to purify and will probably end up as solid waste. Therefore, research is needed to better understand the morphological characteristics of the particles formed by simultaneous crystallization, both when the solid is considered a waste and when it is desired to recover certain components of the solids of economic interest.

It is convenient to classify the studies on simultaneous crystallization according to the solubility of the salts, as moderately soluble salts generate submillimetric particles, whereas slightly soluble salts generate micrometric particles that are more difficult to handle and prone to secondary processes such as polymorphic transformations and

* Corresponding author.
E-mail address: marcelo.seckler@usp.br (M.M. Seckler).

https://doi.org/10.1016/j.desal.2019.114180
Received 26 July 2019; Received in revised form 24 September 2019; Accepted 10 October 2019
Available online 04 November 2019
0011-9164/

Table 1
Conditions for $CaSO_4.0.5H_2O$ seeding experiments.

Experiment	Initial Solution (mol/kg H_2O)		Seed load ($g/kg_{solution}$)
	NaCl	$CaSO_4.0.5H_2O$	$CaSO_4.0.5H_2O$
E1 – Blank	6.725	0.0349	0
E2	6.725	0.0349	1.4
E3	6.725	0.0349	7.0
E4	6.725	0.0349	14

Table 2
Conditions for simultaneous $CaSO_4.0.5H_2O$ and NaCl seeding experiments.

Experiment	Initial Solution (mol/kg H_2O)		Seed load ($g/kg_{solution}$)	
	NaCl	$CaSO_4.0.5H_2O$	NaCl	$CaSO_4.0.5H_2O$
E5	6.691	0.0349	19	–
E6	6.691	0.0349	19	7.0
E7	6.691	0.0349	19	14

aging. Industrial effluents are typically mixtures of moderately and slightly soluble compounds. There are several studies about simultaneous crystallization of poorly soluble salts. For instance, Zieba and Nancollas [11] have studied the coprecipitation of $CaCO_3$ and $SrCO_3$ and reported the influence of ions and of solid surfaces of a single salt on the kinetics and polymorph formation of the other salt. On the other hand, research on the simultaneous crystallization of moderately soluble compounds is much less common. Simultaneous crystallization of a salt and ice has been studied in eutectic freeze context. Ice has been found to crystallize as a single compound that easily separates from several salts by gravity [12–15], but a similar behavior is not expected if ice is not one of the crystallizing compounds. Penha et al. [10,16] have studied the elementary phenomena and the product characteristics during simultaneous crystallization from a NaCl-KCl-H_2O tertiary system in an engineering context. They have found that single crystals yield is favored with NaCl seeding at low supersaturations, i.e. low evaporation rates, small seeds and high seed contents, whilst for KCl seeding single component particles are preferentially formed under high supersaturations, i.e. low seed surface areas (larger seeds in low contents). The authors have concluded that the morphological characteristics of the product may be tuned to yield streams of each compound mainly formed by single component particles, suggesting the feasibility of multicomponent crystallizers for both water and solid reuse. Recently, we have studied the simultaneous crystallization of a moderately and a slightly soluble compound, respectively sodium chloride and calcium sulphate hemihydrate ($CaSO_4.0.5H_2O$) in an unseeded batch evaporative crystallizer [9]. This system was chosen because both compounds are commonly encountered in industrial wastewaters, their simultaneous crystallization being observed in wastewater from an oil refinery [17]. In that contribution, we have found that primary particles of both salts are formed by primary nucleation and grow continuously throughout evaporation. After reaching a certain size, some of the particles agglomerate, yielding a particulate product of multimodal population density, with sizes ranging from 100 to 700 μm. In addition, a considerable amount of $CaSO_4.0.5H_2O$ is in the smaller size ranges. We have also found that low supersaturation (attained under low evaporation rate) hinders agglomeration, yielding a more uniformly sized product.

The solids concentration is an important parameter in crystallization from solutions, as it largely determines the supersaturation, which controls nucleation (primary and secondary), crystal growth and agglomeration [18]. In simultaneous crystallization, the solids content influences additional phenomena, such as heterogeneous nucleation of one phase on the surface of the other one and agglomeration of the compounds with each other [10,16]. In evaporative simultaneous crystallization, the concentration of each solid phase is related to its concentration in the wastewater and its solubility. For the $CaSO_4.0.5H_2O$-NaCl system, the latter is more abundant but there is a range of concentrations of interest. Besides, in industrial configuration the solids contents may be tuned to optimize the particulate morphology, e.g. by seeding in batch processes and by the hydrodynamic design of the crystallizer. In this paper, we extend out previous study to consider the effect of the concentrations of the two solid compounds, $CaSO_4.0.5H_2O$ and NaCl, on elementary phenomena of crystallization and on the particulate product morphology, since these are key parameters to ease solid-liquid separation and to recover valuable components of the wastewater.

2. Methods

Crystallization experiments were conducted by the evaporative method in batch mode in a 0.6 L crystallizer with the NaCl-$CaSO_4$-H_2O ternary system, seeded either with $CaSO_4.0.5H_2O$ alone or with both $CaSO_4.0.5H_2O$ and NaCl. The experimental setup is described in detail in our previous work [9]. The procedure is described below.

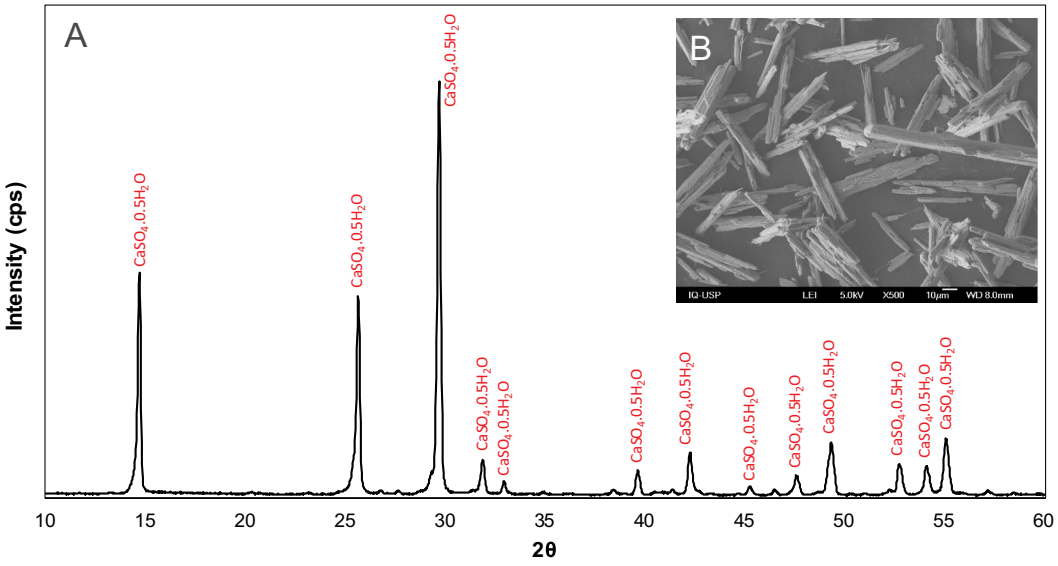

Fig. 1. Diffractogram (A) and a SEM image (B) of $CaSO_4.0.5H_2O$ seeds.

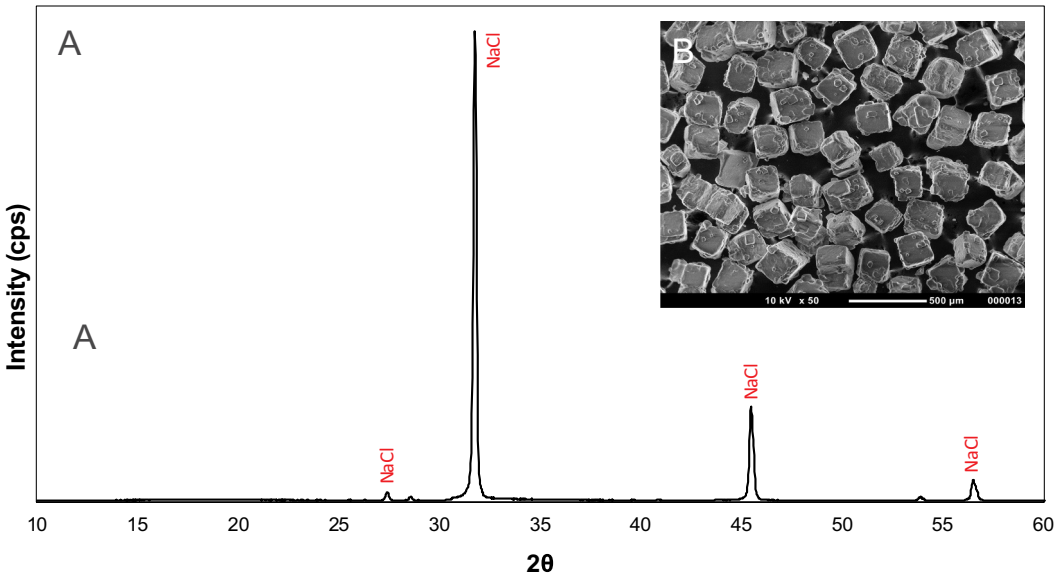

Fig. 2. Diffractogram (A) and a SEM image (B) of NaCl seeds.

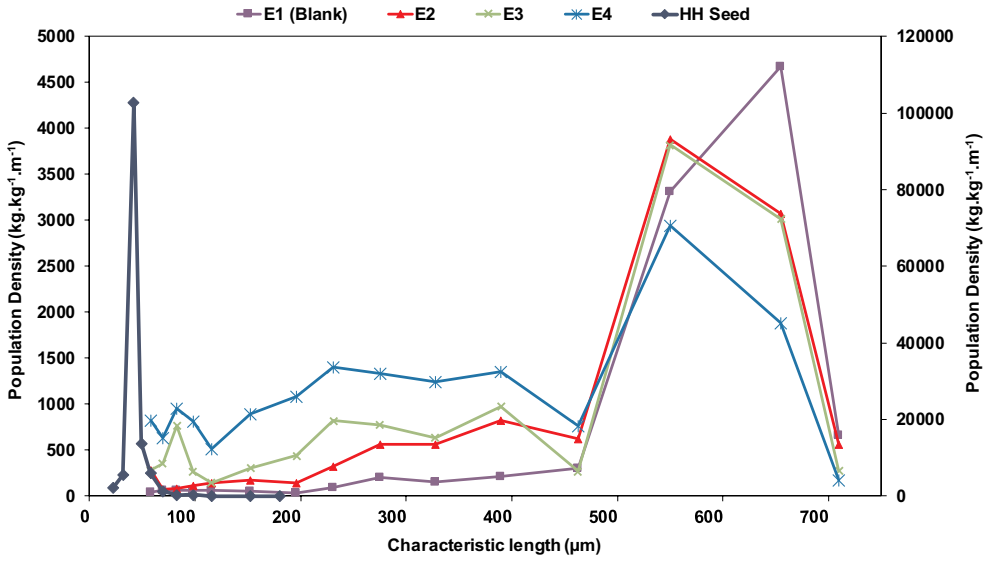

Fig. 3. PSD for experiments with different loads of $CaSO_4.0.5H_2O$ seed: no seed (E1), 1.4 (E2), 7.0 (E3) and 14 g / $kg_{solution}$ (E4) (primary axis). PSD of seeds (secondary axis).

Table 3
Seed load and product characteristics.

Experiment	Seed load (g/ $kg_{solution}$)	Dominant size (µm)	Mass-based mean size ($L_{4,3}$) (µm)	Coefficient of variation (C.V.) (%)
E1 (blank)	–	612	561	8
E2	1.4	596	482	18
E3	7.0	596	426	25
E4	14.0	591	337	38

2.1. $CaSO_4.0.5H_2O$ seeding experiments

Experiment E1 was conducted as a blank, that is, unseeded. In experiments E2, E3 and E4, the amount of seeds added was varied as shown in Table 1.

The initial solution was undersaturated with respect to both salts at 105 °C (slightly below the boiling point of 106 °C) to assure full dissolution of the solid reactants. The desired amount of $CaSO_4.0.5H_2O$ seeds was added (see Table 1) and the suspension was stirred for 15 min for separation of possible particle aggregates. Substantial seeds dissolution is unlikely to occur given the known slow dissolution rates of calcium sulphate hydrates and other slightly soluble salts [19–22]. Seeds dissolution was not substantial as suggested by visual observation of a constant turbidity of the suspension. Thereafter, the temperature of the crystallizer jacket was adjusted to yield the desired evaporation rate. The experiment was conducted until 50% of initial amount of water evaporated. Slurry samples were pippeted after evaporation of 5% and 50% of the initial amount of water, the first one after formation of NaCl particles (visually observed) and the latter at end of the batch. The samples were vacuum filtered, washed with anhydrous ethanol and dried at 50 °C for 12 h.

2.2. Simultaneous $CaSO_4.0.5H_2O$ and NaCl seeding experiments

Three experiments (E5, E6 and E7) were conducted in the presence

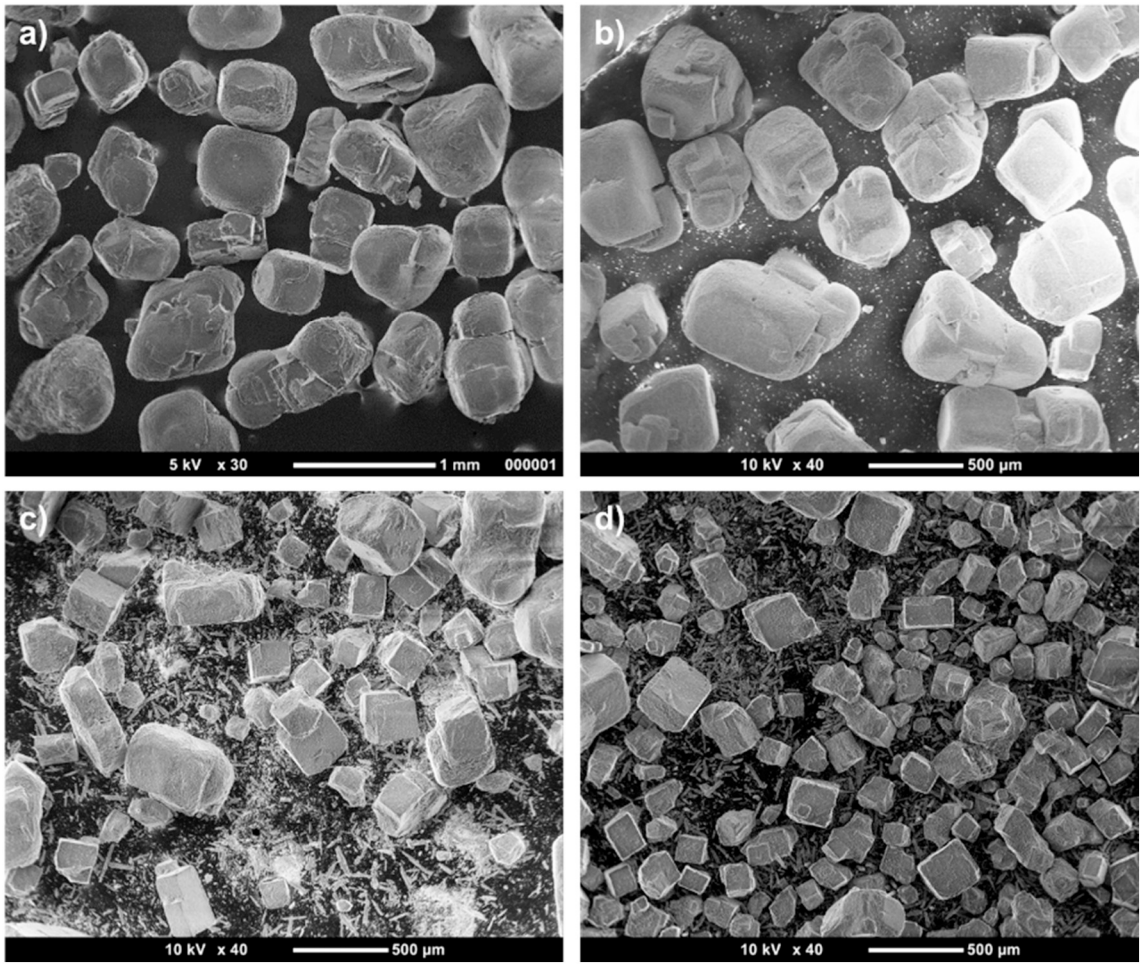

Fig. 4. SEM views of the product from unseeded batch (a) and from batches seeded with $CaSO_4.0.5H_2O$ seed loads (in $g/kg_{solution}$) of 1.4 (b), 7 (c) and 14 (d), respectively, experiments E1, E2, E3 and E4. Magnifications as indicated at the bottom of the figures.

of different loads of $CaSO_4.0.5H_2O$ and a single load of NaCl seeds as shown in Table 2. Experiment E5 was conducted as a blank, that is, only with NaCl seeds.

As before, the initial solution was undersaturated with respect to NaCl and $CaSO_4.0.5H_2O$ at 100 °C. The initial NaCl solution concentration was chosen to yield partial dissolution of the NaCl seeds as explained next. NaCl seeds were added and the suspension was heated to 105 °C, just below the boiling temperature, and kept under stirring for 1 h for NaCl seeds "healing". The "healing" procedure was aimed at the dissolution of a small amount of the NaCl seeds in order to remove any remaining fines and fragments adhered to the crystal surfaces, as well as to allow reconstruction of the corners and correction of irregularities on the crystals. Thereafter, $CaSO_4.0.5H_2O$ seeds were added and the suspension was stirred for 15 min to allow separation of possible particle aggregates.

The experiments were conducted until the removal of 30% of the initial water mass. Samples were taken after evaporation of 5% of the initial amount of water and at end of the batches.

2.3. Seeds preparation

$CaSO_4.0.5H_2O$ seeds were synthesized as described by Feldmann [23]. Initially, 1 L of 4 $mol.L^{-1}$ $CaCl_2.2H_2O$ was added to a vertical cylindrical jacketed glass crystallizer. The solution was heated to 80 °C and kept under stirring for 1 h. Within 4 h, 500 mL of 6.4 $mol.L^{-1}$ H_2SO_4 were added using a peristaltic pump (GILSON MINIPULS® 3). Thereafter the slurry was allowed to equilibrate under the same stirring and temperature for 2 h. The product was vacuum filtered and washed with 3 L of boiling distilled water and subsequently with 0.5 L of isopropanol at room temperature. The product was allowed to dry at 50 °C overnight. Afterwards, the particles were separated by sieving during one hour. Seeds with mean size of 41.5 µm obtained by sieving were used.

NaCl seeds were obtained by sieving analytical grade salt in the size ranges of interest with Tyler series sieves as before. Seeds with mean size of 231 µm were used.

2.4. Particle characterization

Particle shapes were characterized by optical microscopy (Olympus® BX60F-3) and scanning electron microscopy (SEM, JEOL JSM-7401F) and the morphology's of the crystalline lattices were determined by X-ray diffraction (Rigaku Miniflex®). Products chemical composition in terms of calcium content were determined by ICP-OES (Spectro Arcos). The characterization protocol is better described in our previous work [9].

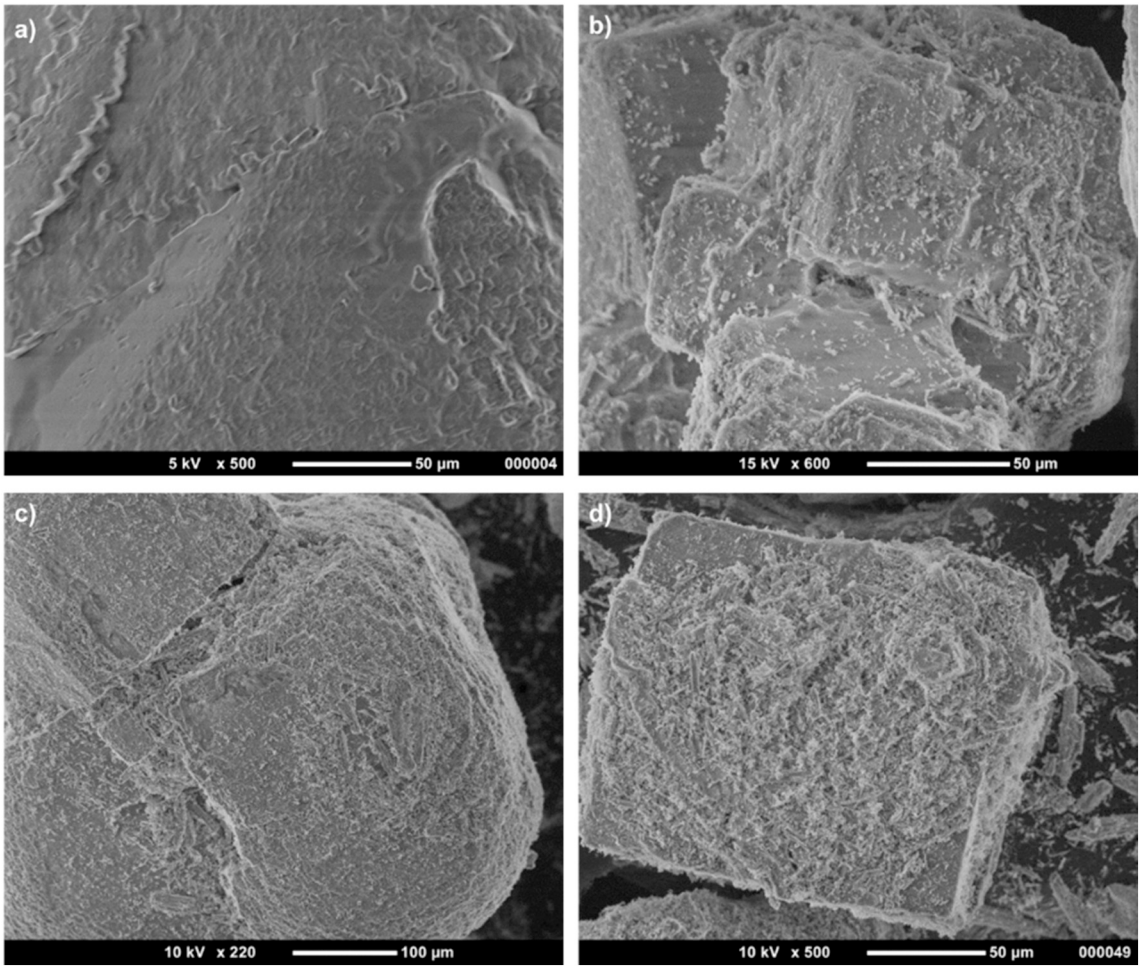

Fig. 5. SEM of the particles for experiments with different loads of $CaSO_4.0.5H_2O$ seed: E1 (a), E2 (b), E3 (c) and E4 (d).

Particle size distributions were determined as mass-based population densities by sieving. The mean particle size was described with the mass-weighed size ($L_{4,3}$) and the width of the distribution with the coefficient of variation (CV) defined from L_{16}, L_{50} and L_{84}, the cumulative characteristic sizes of 16, 50 and 84% of the sample in mass, as shown below.

$$CV = 100.\ \frac{(L_{84} - L_{16})}{2.\ L_{50}} \quad (1)$$

3. Results and discussion

3.1. Seeds characterization

Comparison of the x-ray diffractogram of the calcium sulphate seeds shown in Fig. 1A with the reference pattern [24] shows that they are comprised of $CaSO_4.0.5H_2O$. In addition, the SEM image at Fig. 1B reveals that the primary particles are elongated, which is a characteristic habit of $CaSO_4.0.5H_2O$ crystals [25,26].

Fig. 2A shows the x-ray diffractogram of NaCl seeds, which corresponds to the reference pattern from literature for halite [27]. NaCl seeds observed by SEM in Fig. 2B are predominantly single crystals of cubic habit.

3.2. Main crystallization events

The initial solution is undersaturated with respect to both NaCl and $CaSO_4.0.5H_2O$. In an unseeded batch, water evaporates until the metastable limit of NaCl is reached, triggering primary nucleation and subsequent crystal growth of NaCl from the ternary solution. $CaSO_4.0.5H_2O$ primary nucleation starts later in the batch, possibly influenced by solid NaCl, after the eutonic condition is reached, i.e. the solution in the ternary system is supersaturated with respect to salts of both solutes [28]. Thereafter the solution composition is invariant and both solids continue to form, with possible interaction between solid phases. A mass balance for such a process has been presented in detail in our previous publication [9]. In a $CaSO_4.0.5H_2O$ seeded batch, the $CaSO_4.0.5H_2O$ particles are present before NaCl saturation, so more possibilities arise for solid-solid interactions. Although the solution is undersaturated with respect to $CaSO_4.0.5H_2O$ during part of the batch,

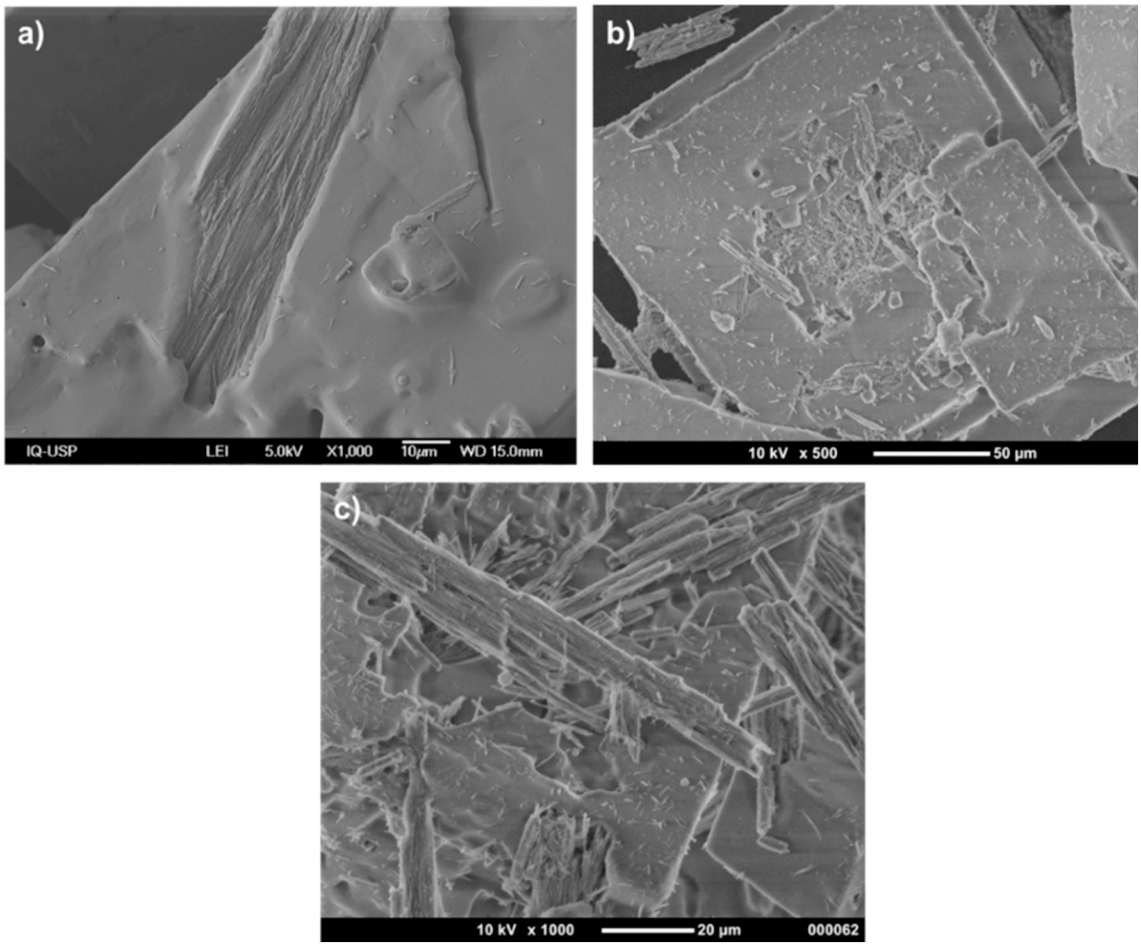

Fig. 6. SEM views of the surfaces of samples with 5% of evaporation extension for the experiments carried out with different $CaSO_4.0.5H_2O$ seed loads: E2 (a), E3 (b) e E4 (c).

$CaSO_4.0.5H_2O$ seeds do not dissolve readily because of their low solubility. For the batches seeded with both salts, NaCl and $CaSO_4.0.5H_2O$, solid-solid interactions are expected from the start of the batch. The nature of the solution-solid and solid-solid interactions is the object of this contribution.

3.3. Effect of $CaSO_4.0.5H_2O$ seeding

The PSDs of the product and of the $CaSO_4.0.5H_2O$ seeds are shown in Fig. 3, mean values and size dispersions (CVs) are given in Table 3. The products PSDs display dominant sizes of about 600 µm. For the unseeded condition (experiment E1) population densities for sizes below 400 µm are unimportant, whereas in the presence of seeds (experiments E2, E3 and E4) the density of particles smaller than 400 µm is also significant. Consequently, $CaSO_4.0.5H_2O$ seeds yields products with smaller mass-based mean sizes and higher size dispersions (higher CV values), in comparison with the unseeded condition.

For the highest $CaSO_4.0.5H_2O$ seed loads (E3 and E4), the PSD also displays a small peak in the 60–120 µm size range. It is likely that it corresponds somehow to $CaSO_4.0.5H_2O$ seeds, which were originally 42 µm in size (Fig. 3). As $CaSO_4.0.5H_2O$ crystals, due to their low solubility, are unlikely to grow more than a few microns in size by a molecular mechanism, the 60–120 µm peak is probably constituted by $CaSO_4.0.5H_2O$ seeds after agglomeration with larger NaCl particles. This issue will be further considered later.

SEM views of the products are shown in Fig. 4. Energy dispersive spectrometry examination (not shown) has confirmed our earlier findings [9] that the acicular crystals correspond to hemihydrate and cubic crystals are sodium chloride. The product is a mixture of small, intermediate, and large particles. The small particles display the acicular habit characteristic of $CaSO_4.0.5H_2O$. Their proportion increases with the $CaSO_4.0.5H_2O$ seed load. Their presence implies that they are ineffective or do not act as a heterogeneous centers for NaCl primary nucleation (otherwise the NaCl heterogeneous nuclei would engulf them upon growth), as already concluded in our previous work [9]. Particles of intermediate size are mainly primary particles of cubic habit, whereas the large particles are either single cubic crystals or agglomerates of these cubic crystals. Given the cubic symmetry of the

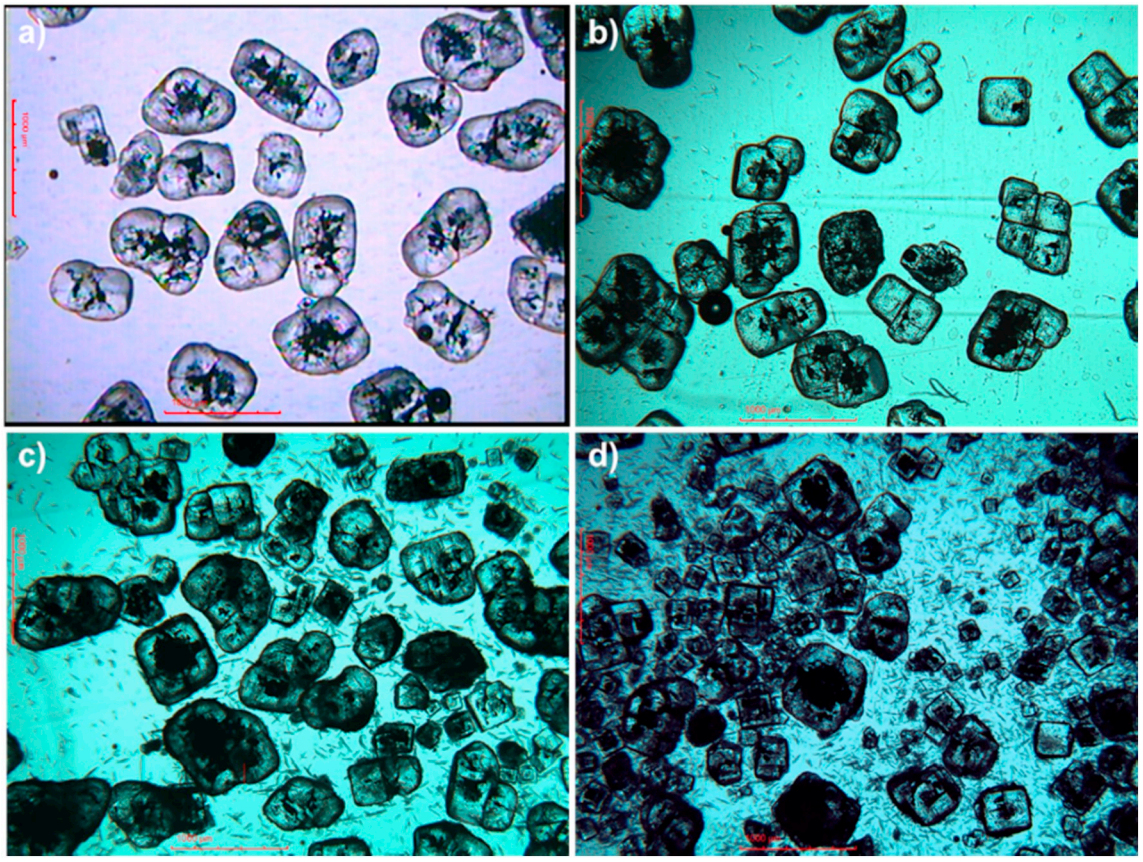

Fig. 7. Optical microscopy images for the experiments carried out with different loads of $CaSO_4.0.5H_2O$ seeds: E1 (a), E2 (b), E3 (c) e E4 (d).

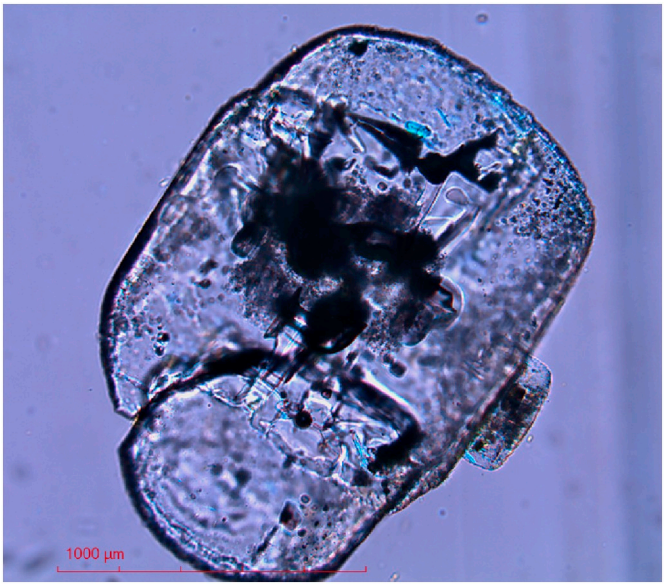

Fig. 8. Optical microscopy of a single particle showing abundant fluid inclusions.

halite crystal lattice, it may be concluded that the intermediate and the large sized particles are either single crystals or agglomerates of NaCl. As the $CaSO_4.0.5H_2O$ seeds load increases (E3 and E4), the proportion of agglomerates in the large size range decreases and the proportion of intermediate sized single crystals becomes more significant, suggesting that $CaSO_4.0.5H_2O$ seeding hampers NaCl agglomeration. This phenomenon is consistent with the product PSDs (Fig. 3), which shows that more seeds results in a larger population density in the intermediate size range.

In order to understand the effect of the $CaSO_4.0.5H_2O$ seeds on NaCl crystallization, it is instructive to consider the particles surfaces in more detail, as Fig. 5 shows. Small needlelike $CaSO_4.0.5H_2O$ particles are attached to the surface of NaCl crystals, forming agglomerates. The same behaviour has been observed before for unseeded NaCl – $CaSO_4.0.5H_2O$ simultaneous crystallization [9]. It is hypothesized that these tiny $CaSO_4.0.5H_2O$ particles on the surface of NaCl crystals mechanically inhibits the agglomeration between crystals of NaCl. This effect is more prominent as the seed load increases because the amount of $CaSO_4.0.5H_2O$ crystals on the NaCl surfaces also increases.

As the NaCl crystal growth rate is higher than the growth rate of calcium sulphate [25,29], $CaSO_4.0.5H_2O$ particles on the NaCl surface are engulfed by the growing NaCl crystal and eventually incorporated into it. The SEM views of Fig. 6 shows partly “buried” particles. They increase in importance as the $CaSO_4.0.5H_2O$ seed load increases.

Optical microscopies of the particulate products are shown in Fig. 7. The overall appearance of the particles is consistent with the SEM views shown in Fig. 4: the product is comprised of small $CaSO_4.0.5H_2O$ needles, intermediate sized single NaCl particles and large agglomerates, with the proportion of agglomerates decreasing and the size dispersion increasing with increasing $CaSO_4.0.5H_2O$ seed load. Fig. 8 shows a single particle with higher magnification. Abundant fluid inclusions are

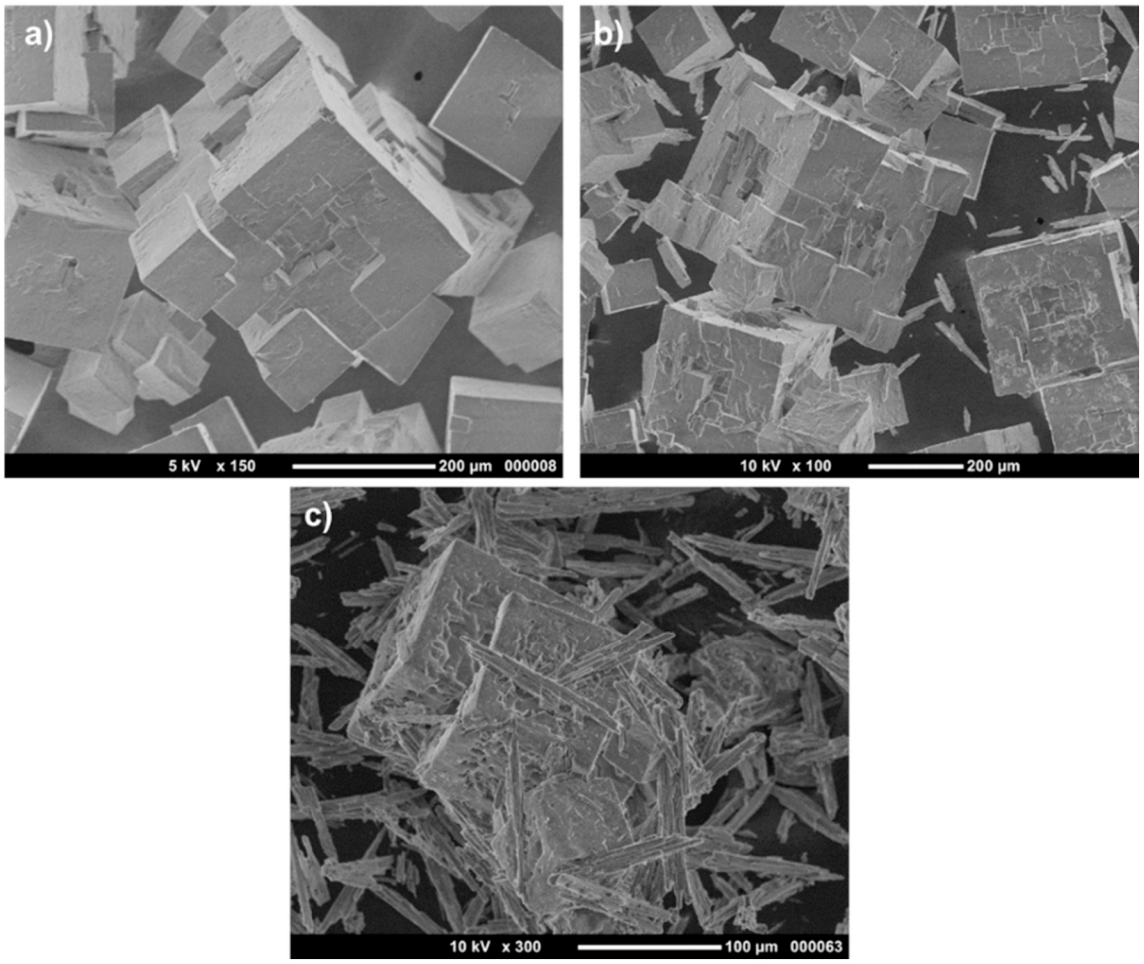

Fig. 9. SEM of the samples with 5% of evaporation extension water evaporated for the experiments carried out with different $CaSO_4.0.5H_2O$ seed loads: E2 (a), E3 (b) e E4 (c).

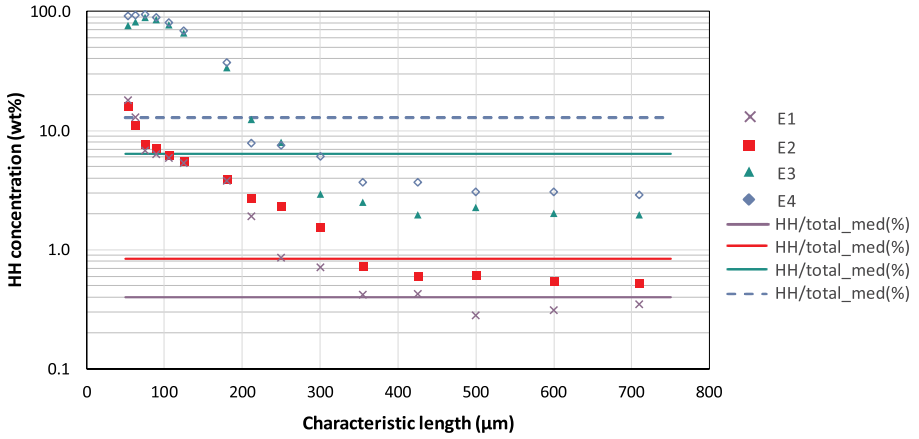

Fig. 10. $CaSO_4.0.5H_2O$ content in the solid product versus particle size for different $CaSO_4.0.5H_2O$ seed loads: E1, E2, E3 e E4. The horizontal lines represent the mean $CaSO_4.0.5H_2O$ content of the product.

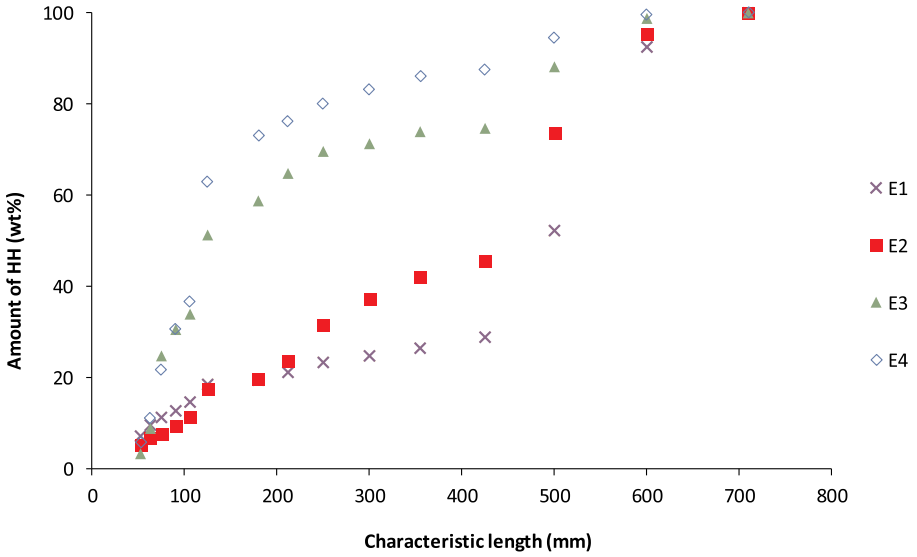

Fig. 11. Cumulative amount of $CaSO_4.0.5H_2O$ produced versus particle size for different $CaSO_4.0.5H_2O$ seed loads (E1, E2, E3 and E4, respectively).

observed. Inclusions appear as rounded droplets within the crystals or as dark areas when they are small or abundant. Fig. 7 shows that such fluid inclusions develop in all conditions investigated and are more prominent for higher seed loads. The development of such fluid inclusions may be understood by inspection of NaCl particles surfaces after 5% of evaporation extension, as shown in Fig. 9. The NaCl crystals display "hopper" habit, which is characterized by a cavity in the center of the crystal faces. Besides, the hopper steps become more irregular as the seed load increases. The hopper habit is known to promote the formation of fluid inclusions upon further crystal growth [9,30]. Rough crystal surfaces are also known to promote fluid inclusions [18,30,31]. It is suggested that $CaSO_4.0.5H_2O$ particles adhered to the growing NaCl surfaces affects the fluid flow field around the crystals, leading to instabilities in the growing NaCl surfaces.

The $CaSO_4.0.5H_2O$ concentration in each particle size range is shown in Fig. 10. Below 200 μm, the highest $CaSO_4.0.5H_2O$ concentrations are observed. The concentration decays exponentially with size up to 400 μm, assuming a constant value above 400 μm. Besides, the $CaSO_4.0.5H_2O$ concentration in the product for all size ranges increases with the $CaSO_4.0.5H_2O$ seed load, corroborating the SEM observations. Thus, even though $CaSO_4.0.5H_2O$ develops in sizes < 30 μm, it is present in the whole size range of the product, which is consistent with the hypothesis of agglomeration between small $CaSO_4.0.5H_2O$ primary particles and NaCl.

The "amount of $CaSO_4.0.5H_2O$" is presented is Fig. 11. This variable represents the distribution of the amount of $CaSO_4.0.5H_2O$ with the product size, and was calculated based on the multiplication of the $CaSO_4.0.5H_2O$ content and the product mass for each size fraction, normalized for a total $CaSO_4.0.5H_2O$ amount of $CaSO_4.0.5H_2O$ of unity. It shows that $CaSO_4.0.5H_2O$ is found in all size ranges. Closer inspection in the figure shows that the product fraction > 400 μm contains about 30% of the $CaSO_4.0.5H_2O$ for high seed load conditions (E3 and E4), but as much as roughly 70% of the $CaSO_4.0.5H_2O$ for low seed load experiments (E1 and E2). This product fraction displays a $CaSO_4.0.5H_2O$ content lower than the mean (see Fig. 10) and corresponds to the primary peak of the PSD (Fig. 3).

3.4. Effect of $CaSO_4.0.5H_2O$ and NaCl seeding

In NaCl-seeded experiments, as the $CaSO_4.0.5H_2O$ seed load increases, a shoulder appears on the left size of the main peak of the PSD, with particle sizes about 400 μm, which eventually becomes a secondary peak for the highest seed load (Fig. 12a). Consequently, the dominant size decreases and the size dispersion increases, as shown in Table 4. A similar behavior was already observed for the NaCl-unseeded experiments, although there the PSDs were bimodal.

The NaCl seeds PSD (Fig. 12b) is not observed in the product PSD, suggesting that NaCl undergoes extensive growth and agglomeration. However, for the $CaSO_4.0.5H_2O$ seeded experiments a population density peak was observed in the smallest size range, which is likely derived from agglomeration of $CaSO_4.0.5H_2O$ seeds with NaCl particles. This feature had already been observed for the NaCl-unseeded experiments.

SEM views of the NaCl-seeded products are shown in Fig. 13. Particles formed without $CaSO_4.0.5H_2O$ seeds (E5) are mainly agglomerates formed by two or three primary crystals of NaCl, whereas $CaSO_4.0.5H_2O$ particles are not observed. As the amount of $CaSO_4.0.5H_2O$ seeds increases, NaCl single crystals also appear in increasing amount next to the agglomerates, whereas $CaSO_4.0.5H_2O$ appears partly as isolated crystals and partly attached to the surface of NaCl particles, as was already observed with NaCl-unseeded experiments.

Sieved fractions of the product with mean sizes of 390 and 550 μm were further investigated by SEM (Fig. 14) and optical microscopy (Fig. 15). It was found that the larger particles are mainly agglomerates formed by two or three primary NaCl crystals, whereas the smaller ones are mainly single crystals. It is likely that these single crystals are mainly seed particles after molecular crystal growth, as a simple calculation shows, considering a seeded batch crystallization in which crystal growth is the only elementary process. The product size is calculated with the following Eq. [18]:

$$L_{prod} = \sqrt[3]{L_{seed}^3 + \frac{\Delta m}{m_{seed}}} \quad (2)$$

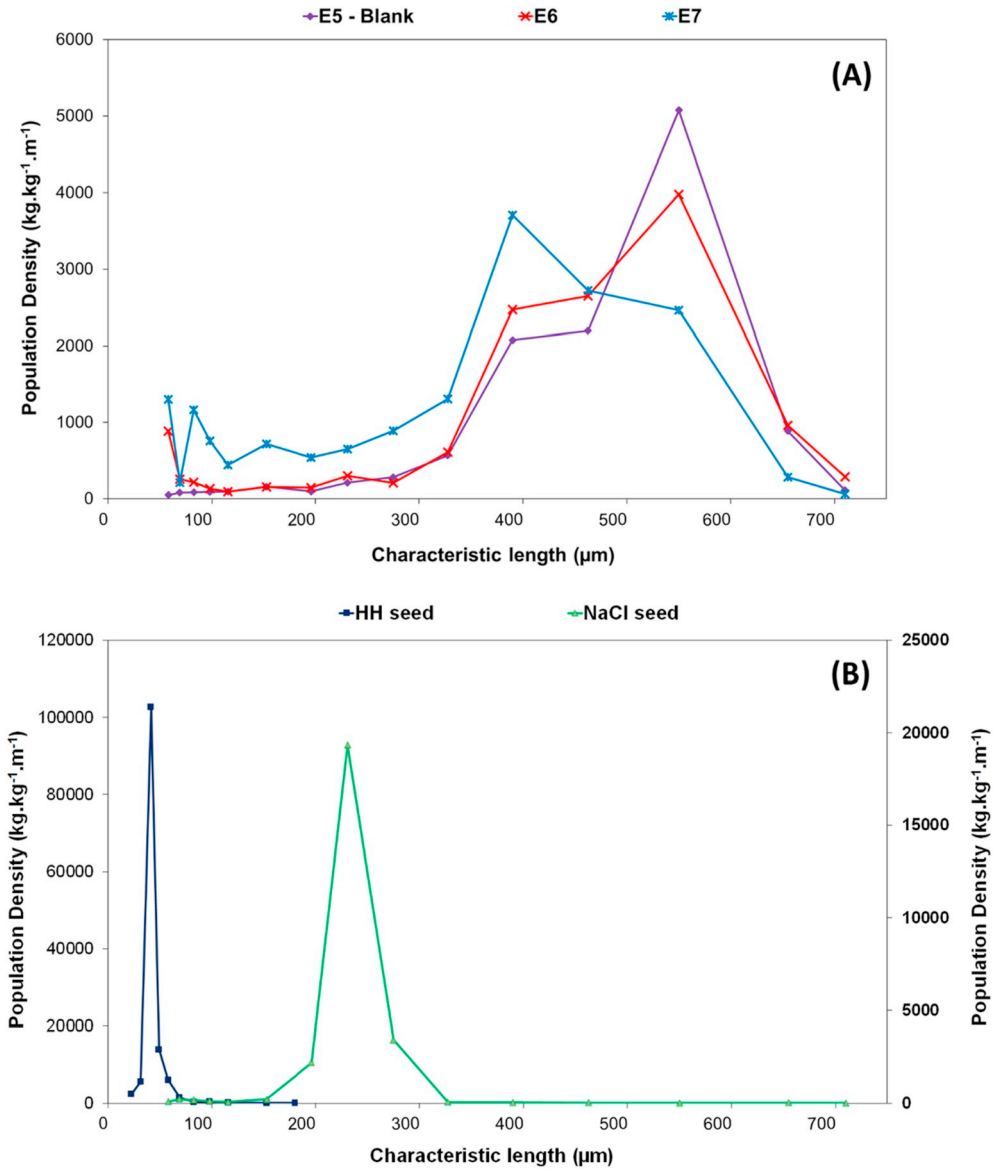

Fig. 12. Product PSD's (a) for experiments with NaCl seeds only (E5 – blank, 19 g/$kg_{solution}$) and seeded with both NaCl (19 g/$kg_{solution}$) and different loads of $CaSO_4.0.5H_2O$, E6 (7 g/$kg_{solution}$) and E7 (14 g/$kg_{solution}$) (b) PSD's of $CaSO_4.0.5H_2O$ seeds (primary axis) and NaCl seeds (secondary axis).

Table 4
Product characteristics.

Experiment	Dominant size (μm)	Mass-based mean particle size ($L_{4,3}$) (μm)	CV (%)
E5	524	463	18
E6	515	437	20
E7	421	344	32

where L_{seed} and L_{prod} are the seed and product mean sizes, Δm and m_{seed} are the crystallized and seed masses. The so calculated product size is approximately 400 μm which is similar to the secondary peak of 390 μm observed in the PSD's.

The product particles formed under the highest seed load (E7) are partly smaller than the grown seeds of 390 μm (Fig. 12a), suggesting that NaCl nucleation takes place during the batch. It is likely that, because of $CaSO_4.0.5H_2O$ agglomeration upon NaCl crystals, the NaCl surface available for crystal growth is reduced, causing a sufficiently high supersaturation for primary nucleation to occur. For low $CaSO_4.0.5H_2O$ seed load or $CaSO_4.0.5H_2O$ – unseeded experiments such nucleation is less evident from the PSDs. SEM views of NaCl crystals with surfaces increasingly covered with $CaSO_4.0.5H_2O$ at increasing $CaSO_4.0.5H_2O$ seed loads are shown in Fig. 16.

$CaSO_4.0.5H_2O$ distribution with particle size in these NaCl-seeded experiments is qualitatively similar to the NaCl-unseeded cases shown

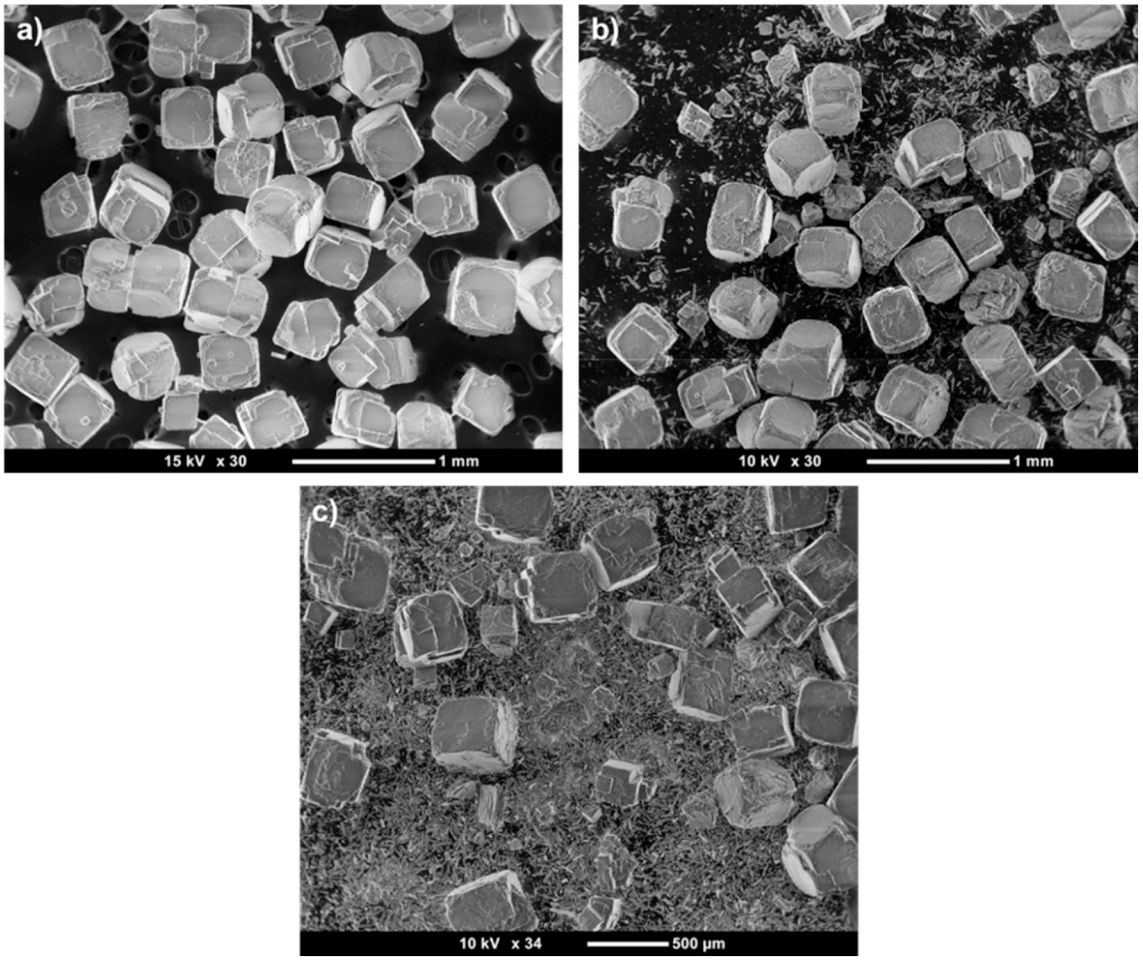

Fig. 13. SEM images for the experiment carried out with NaCl seeds (a) and in the absence of $CaSO_4.0.5H_2O$ seeds - E5; (b) - and the experiments carried out with NaCl seeds and with $CaSO_4.0.5H_2O$ seed loads of 7 g/kg_{prod} (b) – E6 – e 14 g/kg_{prod} (c) – E7.

before, as Figs. 17 and 18 show. However, for NaCl-seeding $CaSO_4.0.5H_2O$ segregation with particle size is more pronounced, particularly for high $CaSO_4.0.5H_2O$ seed load, as the product size fraction > 400 µm has a lower $CaSO_4.0.5H_2O$ content of 1.5% (mean value of E6 and E7) in comparison with 2.6% (mean value of E3 and E4) for NaCl-unseeded conditions. Besides, the amount of $CaSO_4.0.5H_2O$ in this size range is only 12%, against 19% under NaCl-unseeded conditions (mean of E6 and E7 and mean of E3 and E4, respectively).

SEM views of the $CaSO_4.0.5H_2O$ – rich end of the PSD is shown in Fig. 19. For the experiment unseeded in $CaSO_4.0.5H_2O$ only NaCl particles are observed, whereas for the $CaSO_4.0.5H_2O$ seed load of 7 g/kg single crystals of $CaSO_4.0.5H_2O$ needles are prevalent over NaCl particles, whereas for 14 g/kg $CaSO_4.0.5H_2O$ seeds only $CaSO_4.0.5H_2O$ particles are present.

3.5. Potential for application in desalination processes

In simultaneous crystallization of aqueous effluents aiming at zero liquid discharge, it is desirable to obtain large particles and a small size dispersion to facilitate downstream processes such as filtration or centrifugation. In our previous work [9] about unseeded simultaneous crystallization, we have established that, even though $CaSO_4.0.5H_2O$ particles develop in the micrometric size range, the product of simultaneous crystallization with NaCl is submillimetric. We have also concluded that a product of narrow size distribution is favored at a low evaporation rate of 0,002 min^{-1}. In this work, we have increased the amount of $CaSO_4.0.5H_2O$ and NaCl in the system by seeding. The corresponding product is submillimetric as before. Besides, high concentrations of $CaSO_4.0.5H_2O$ seeds (7 and 14 g/kg) yield smaller and more polydispersed particles because $CaSO_4.0.5H_2O$ crystals attach to the surface of NaCl crystals inhibiting agglomeration and sometimes promoting NaCl primary nucleation. Seeding with NaCl favors a moderately lower amount of $CaSO_4.0.5H_2O$ in the > 400 µm size range, which constitutes most of the yield. One concludes that simultaneous crystallization of $CaSO_4.0.5H_2O$ – NaCl, irrespective of $CaSO_4.0.5H_2O$ content, yields a product that is satisfactory for downstream handling. However, seeding with $CaSO_4.0.5H_2O$ is not recommended at it reduces the mean size and increases the size dispersion of the product. NaCl

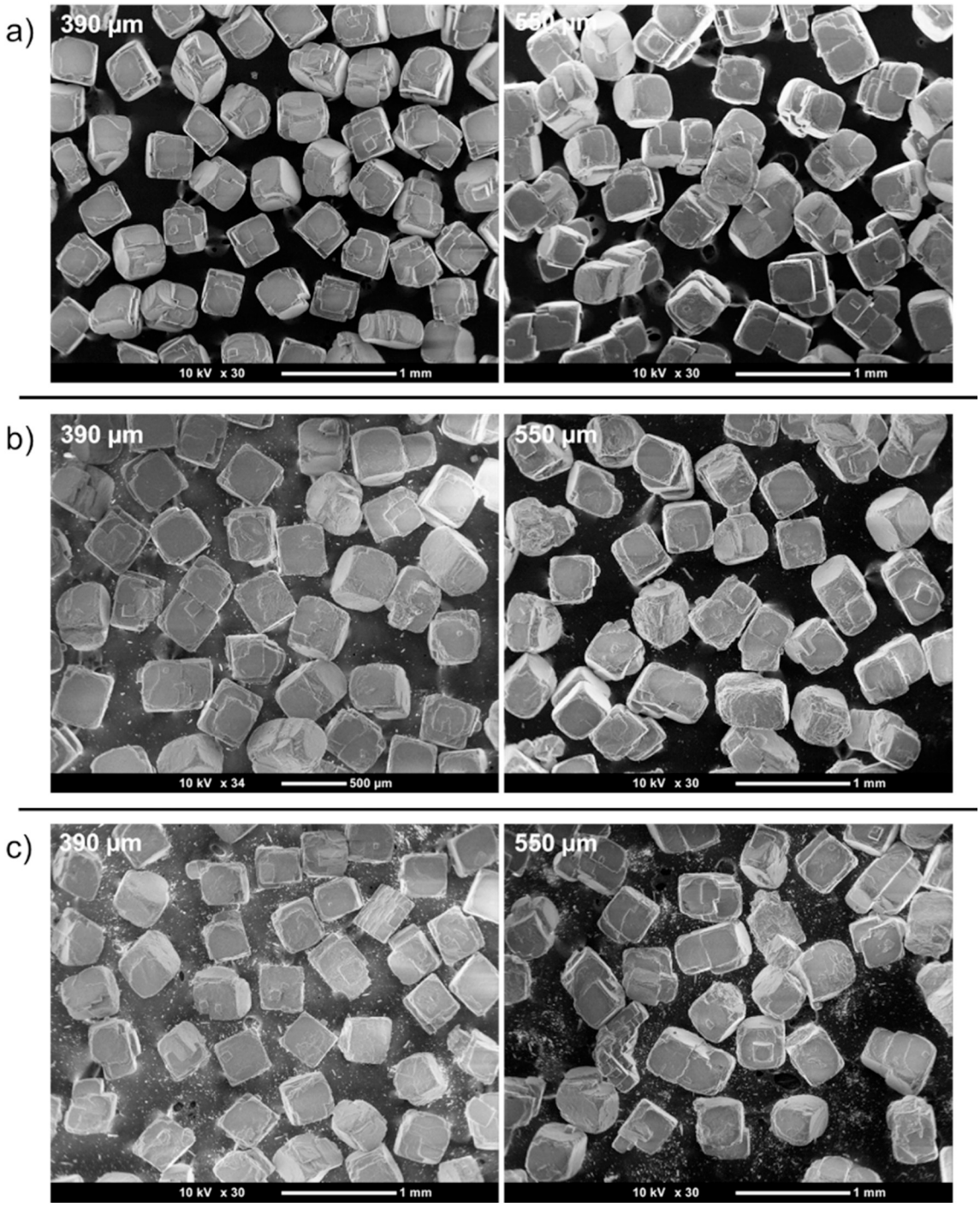

Fig. 14. SEM images of the product of the 390 and 550 µm fraction for the experiment carried out with NaCl seeds and in the absence of hemihydrate (a) - E5 - seeds and the experiments carried out with NaCl seeds and with hemihydrate seed loads of 7 g/kg_{prod} (b) – E6 – e 14 g/kg_{prod} – E7.

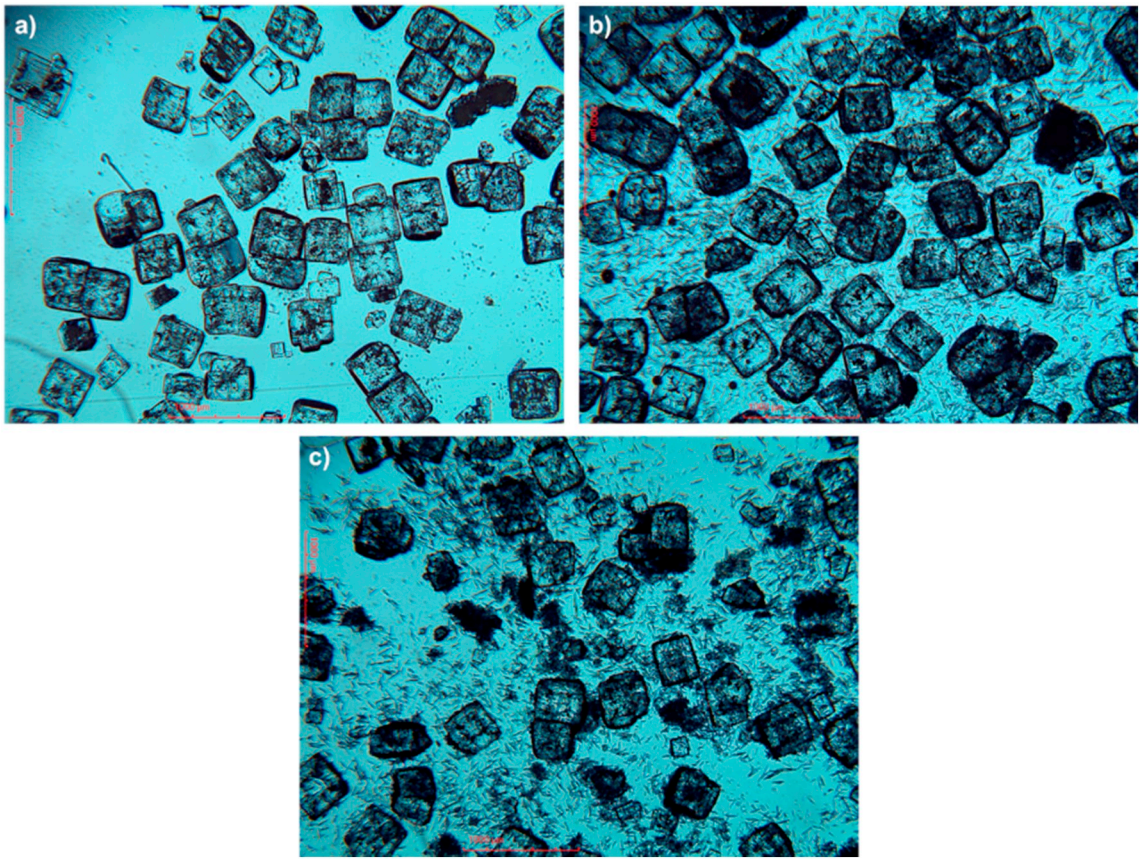

Fig. 15. Optical microscopy images for the experiment carried out with NaCl seeds and in the absence of $CaSO_4.0.5H_2O$ seeds (a) - E5 - and the experiments carried out with NaCl seeds and with $CaSO_4.0.5H_2O$ seed loads of 7 g/kg_{prod} (b) – E6 – e 14 g/kg_{prod} – E7.

seeding may be considered if it is desirable to separate $CaSO_4.0.5H_2O$ from NaCl downstream the crystallizer by size classification.

4. Conclusions

The main elementary processes of seeded batch simultaneous crystallization of sodium chloride and calcium sulphate hemihydrate ($CaSO_4.0.5H_2O$) from aqueous solution at 106 °C are $CaSO_4.0.5H_2O$ crystal growth, NaCl crystal growth, and agglomeration of NaCl particles with each other and with $CaSO_4.0.5H_2O$ particles. In the presence of $CaSO_4.0.5H_2O$ seeds only, NaCl nucleates primarily in solution, not upon $CaSO_4.0.5H_2O$ particles. $CaSO_4.0.5H_2O$ particles adhere to the surface of NaCl crystals and sterically hamper agglomeration of NaCl particles with each other. Besides, such $CaSO_4.0.5H_2O$ particles partly cover NaCl crystal surfaces, reducing the area available for NaCl crystal growth and causing the supersaturation with respect to NaCl to increase. For a sufficiently high $CaSO_4.0.5H_2O$ seed load, primary nucleation of NaCl takes place during the batch. The above phenomena explain the morphological features of the particulate product summarized next.

The particulate product is comprised of single $CaSO_4.0.5H_2O$ crystals in the micrometric size range and particles in the submillimetric size range. The latter are either NaCl single crystals or agglomerates of NaCl composed of a few primary NaCl particles, with $CaSO_4.0.5H_2O$ crystals either attached to their surface or engulfed by the NaCl crystals. $CaSO_4.0.5H_2O$ is distributed throughout all size ranges of the PSD due to its agglomeration with NaCl particles, with higher $CaSO_4.0.5H_2O$ concentrations in the smallest sizes. $CaSO_4.0.5H_2O$ seeding favors the formation of smaller and more polydispersed particles. Both $CaSO_4.0.5H_2O$ and NaCl seeding favor a product with $CaSO_4.0.5H_2O$ mainly in the smaller sized particles of the PSD.

If applied to aqueous effluents aiming at zero liquid discharge, simultaneous crystallization of $CaSO_4.0.5H_2O$ and NaCl yields a product that is satisfactory for downstream handling even for high $CaSO_4.0.5H_2O$ content in the crystallizer. However, seeding with $CaSO_4.0.5H_2O$ is not recommended at it reduces the mean size and increases the size dispersion of the product. NaCl seeding may be considered if it is desirable to separate $CaSO_4.0.5H_2O$ from NaCl downstream the crystallizer by size classification, as it favors $CaSO_4.0.5H_2O$ to end up in smaller size fractions of the product.

Declaration of Competing Interest.

The authors declare no competing interests.

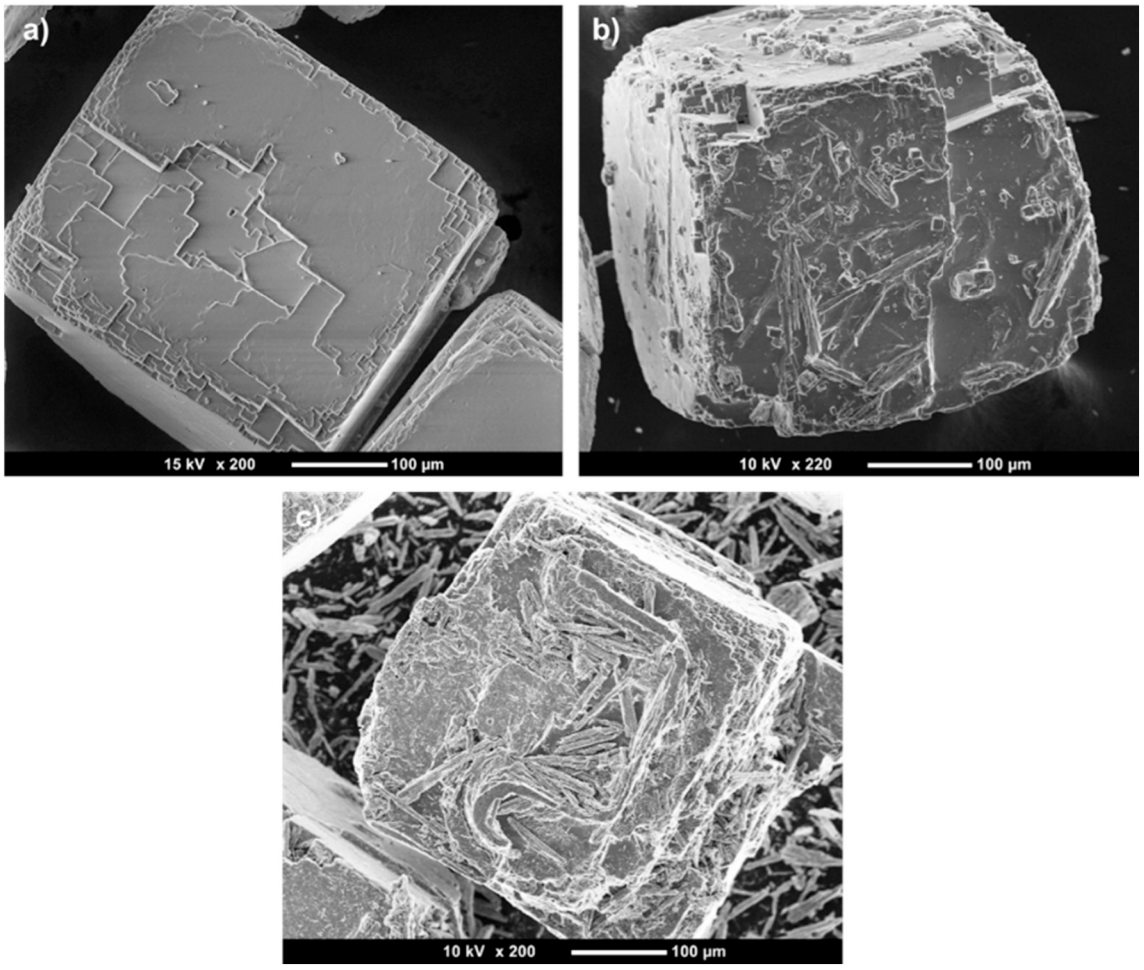

Fig. 16. SEM views of the surface of the product of the experiment carried out with NaCl seeds and in the absence of $CaSO_4.0.5H_2O$ seeds (a) - E5 - and the experiments carried out with NaCl seeds and $CaSO_4.0.5H_2O$ seed loads of 7 g/kg_{prod} (b) – E6 – e 14 g/kg_{prod} – E7.

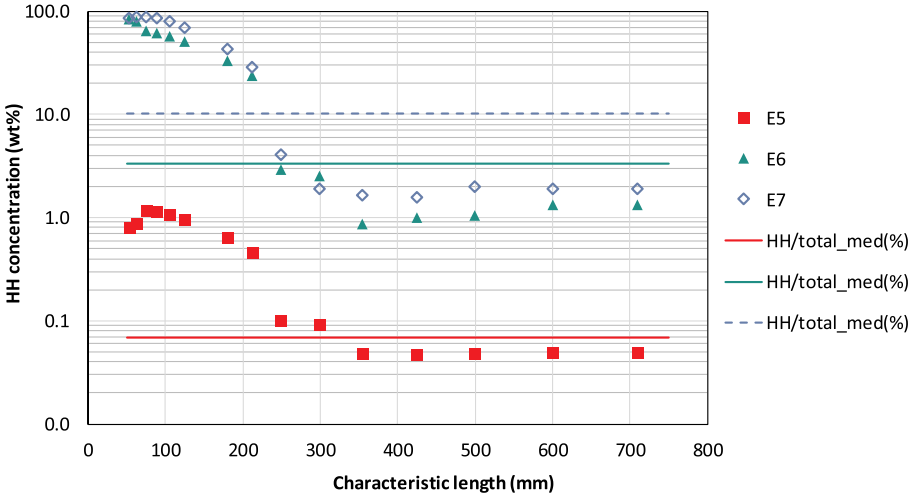

Fig. 17. $CaSO_4.0.5H_2O$ content in the solid product versus particle size for the blank - E5 - and the experiments carried out with NaCl seeds and with $CaSO_4.0.5H_2O$ seed loads of 7 g/kg_{prod} – E6 – e 14 g/kg_{prod} – E7. The horizontal lines represent the mean $CaSO_4.0.5H_2O$ content of the product.

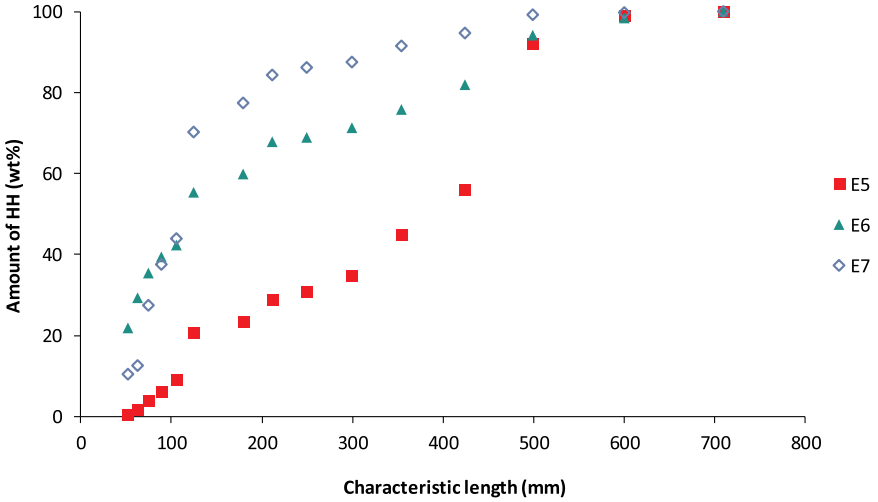

Fig. 18. Cumulative amount of $CaSO_4.0.5H_2O$ produced versus particle size for the blank - E5 - and the experiments carried out with NaCl seeds and with $CaSO_4.0.5H_2O$ seed loads of 7 g/kg_{prod} – E6 – e 14 g/kg_{prod} – E7.

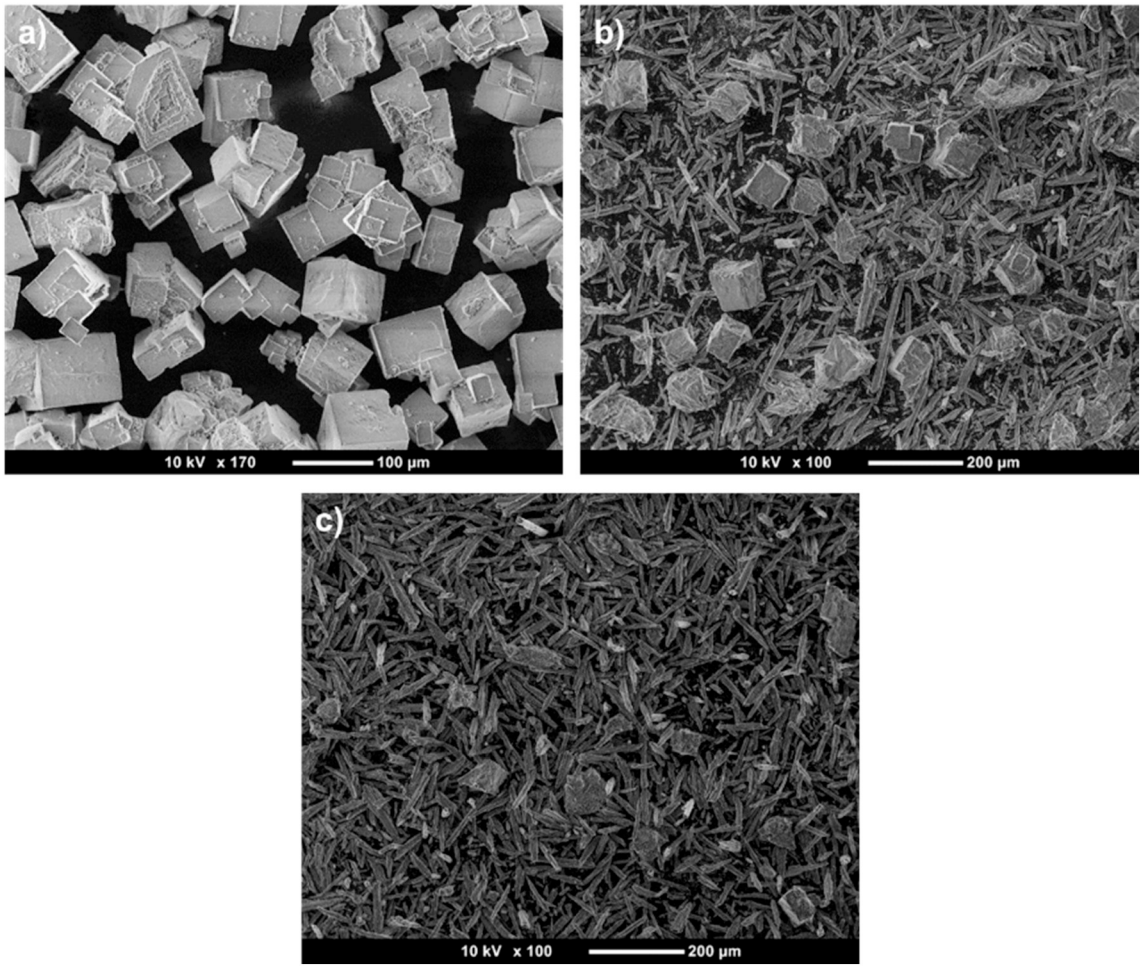

Fig. 19. SEM views of the product particles in the size range of 58 to 83 µm (a) for the blank - E5 - and the experiments with NaCl seeds and $CaSO_4.0.5H_2O$ seed loads of 7 g / kg_{prod} (b) - E6 - and 14 g / kg_{prod} (c) - E7.

Acknowledgements

The financial support of the National Council for Scientific and Technological Development (CNPq), of the Coordination for the Improvement of Higher Education Personnel (CAPES) and of Petrobras are gratefully acknowledged.

References

[1] S. Ahirrao, Chapter 13 - Zero Liquid Discharge Solutions, in: V.V. Ranade, V.M. Bhandari (Eds.), Ind. Wastewater Treat. Recycl. Reuse, Butterworth-Heinemann, Oxford, 2014, pp. 489–520, , https://doi.org/10.1016/B978-0-08-099968-5.00013-1.

[2] K.J. Lu, Z.L. Cheng, J. Chang, L. Luo, T.-S. Chung, Design of zero liquid discharge desalination (ZLDD) systems consisting of freeze desalination, membrane distillation, and crystallization powered by green energies, Desalination 458 (2019) 66–75, https://doi.org/10.1016/j.desal.2019.02.001.

[3] L.M. Vane, Water recovery from brines and salt-saturated solutions: operability and thermodynamic efficiency considerations for desalination technologies, J. Chem. Technol. Biotechnol. 92 (2017) 2506–2518, https://doi.org/10.1002/jctb.5225.

[4] C.E. Pantoja, Y.N. Nariyoshi, M.M. Seckler, Membrane distillation crystallization applied to brine desalination: a hierarchical design procedure, Ind. Eng. Chem. Res. 54 (2015) 2776–2793, https://doi.org/10.1021/ie504695p.

[5] X. Jiang, L. Tuo, D. Lu, B. Hou, W. Chen, G. He, Progress in membrane distillation crystallization: process models, crystallization control and innovative applications, Front. Chem. Sci. Eng. (2017), https://doi.org/10.1007/s11705-017-1649-8.

[6] D.G. Randall, J. Nathoo, A.E. Lewis, A case study for treating a reverse osmosis brine using eutectic freeze crystallization—approaching a zero waste process, Desalination 266 (2011) 256–262, https://doi.org/10.1016/j.desal.2010.08.034.

[7] G. Guan, C. Yao, S. Lu, Y. Jiang, H. Yu, X. Yang, Sustainable operation of membrane distillation for hypersaline applications: roles of brine salinity, membrane permeability and hydrodynamics, Desalination 445 (2018) 123–137, https://doi.org/10.1016/j.desal.2018.07.031.

[8] D.H. Kim, A review of desalting process techniques and economic analysis of the recovery of salts from retentates, Desalination 270 (2011) 1–8, https://doi.org/10.1016/j.desal.2010.12.041.

[9] G.P. Zago, F.M. Penha, M.M. Seckler, Product characteristics in simultaneous crystallization of NaCl and CaSO4 from aqueous solution under different evaporation rates, Desalination 457 (2019) 85–95, https://doi.org/10.1016/j.desal.2019.01.021.

[10] F.M. Penha, G.P. Zago, Y.N. Nariyoshi, A. Bernardo, M.M. Seckler, Simultaneous crystallization of NaCl and KCl from aqueous solution: elementary phenomena and product characterization, Cryst. Growth Des. 18 (2018) 1645–1656, https://doi.org/10.1021/acs.cgd.7b01603.

[11] A. ZIEBA, G.H. NANCOLLAS, Constant composition kinetics studies of the simultaneous CRYSTAL-growth of alkaline-earth carbonates - the calcium strontium system, J. Cryst. Growth 144 (1994) 311–319, https://doi.org/10.1016/0022-0248(94)90472-3.

[12] R.J.C. Vaessen, B.J.H. Janse, M.M. Seckler, G.J. Witkamp, Evaluation of the performance of a newly developed eutectic freeze crystallizer: scraped Cooled Wall CrystalIizer, Chem. Eng. Res. Des. 81 (2003) 1363–1372, https://doi.org/10.1205/026387603771339573.

[13] A.E. Lewis, J. Nathoo, K. Thomsen, H.J. Kramer, G.J. Witkamp, S.T. Reddy, D.G. Randall, Design of a Eutectic Freeze Crystallization process for multi-component waste water stream, Chem. Eng. Res. Des. 88 (2010) 1290–1296, https://doi.org/10.1016/j.cherd.2010.01.023.

[14] M. Hasan, N. Rotich, M. John, M. Louhi-Kultanen, Salt recovery from wastewater by air-cooled eutectic freeze crystallization, Chem. Eng. J. 326 (2017) 192–200, https://doi.org/10.1016/j.cej.2017.05.136.

[15] S.T. Reddy, A.E. Lewis, G.J. Witkamp, H.J.M. Kramer, J. van Spronsen, Recovery of Na2SO4 center dot 10H(2)O from a reverse osmosis retentate by eutectic freeze crystallisation technology, Chem. Eng. Res. Des. 88 (2010) 1153–1157, https://doi.org/10.1016/j.cherd.2010.01.010.

[16] F.M. Penha, G.P. Zago, M.M. Seckler, STRATEGIES TO CONTROL PRODUCT CHARACTERISTICS IN SIMULTANEOUS CRYSTALLISATION OF NaCl AND KCl FROM AQUEOUS SOLUTION: SEEDING WITH KCl, Cryst. Growth Des. (2019), https://doi.org/10.1021/acs.cgd.8b01670.

[17] E. Mayer, A. Becheleni, R.P. Borba, M.M. Seckler, Water recovery from saline streams produced by electrodialysis, Environ. Technol. 36 (2014) 386–394, https://doi.org/10.1080/09593330.2014.978898.

[18] A. Lewis, M. Seckler, H. Kramer, G. van Rosmalen, Industrial Crystallization, Cambrige University Press, Cambridge, United Kingdom NV - 323, 2015.

[19] F. Brandt, D. Bosbach, Bassanite (CaSO4·0.5H2O) dissolution and gypsum (CaSO4·2H2O) precipitation in the presence of cellulose ethers, J. Cryst. Growth 233 (2001) 837–845, https://doi.org/10.1016/S0022-0248(01)01637-2.

[20] S.-T. Liu, G.H. Nancollas, The kinetics of dissolution of calcium sulfate dihydrate, J. Inorg. Nucl. Chem. 33 (1971) 2311–2316, https://doi.org/10.1016/0022-1902(71)80205-1.

[21] M.M. Mbogoro, M.E. Snowden, M.A. Edwards, M. Peruffo, P.R. Unwin, Intrinsic kinetics of gypsum and calcium sulfate anhydrite dissolution: surface selective studies under hydrodynamic control and the effect of additives, J. Phys. Chem. C 115 (2011) 10147–10154, https://doi.org/10.1021/jp201718b.

[22] L. Amathieu, R. Boistelle, Crystallization kinetics of gypsum from dense suspension of hemihydrate in water, J. Cryst. Growth 88 (1988) 183–192, https://doi.org/10.1016/0022-0248(88)90275-8.

[23] T. Feldmann, Crystallization Kinetic Investigations of Calcium Sulfate Phases in Aqueous CaCl2-HCl Solutions, McGill University, 2013.

[24] A.N. Christensen, T.R. Jensen, A. Nonat, A new calcium sulfate hemi-hydrate, Dalt. Trans. 39 (2010) 2044–2048, https://doi.org/10.1039/b913648g.

[25] T. Feldmann, G.P. Demopoulos, The crystal growth kinetics of alpha calcium sulfate hemihydrate in concentrated CaCl2–HCl solutions, J. Cryst. Growth 351 (2012) 9–18, https://doi.org/10.1016/j.jcrysgro.2012.04.014.

[26] B. Kong, B. Guan, M.Z. Yates, Z. Wu, Control of α - Calcium Sulfate Hemihydrate Morphology Using Reverse Microemulsions, (2012), pp. 8–13.

[27] P. Fontana, J. Schefer, D. Pettit, Characterization of sodium chloride crystals grown in microgravity, J. Cryst. Growth 324 (2011) 207–211, https://doi.org/10.1016/j.jcrysgro.2011.04.001.

[28] H. DeVoe, Thermodynamics and Chemistry, Prentice Hall, 2001, https://books.google.com.br/books?id=VnIvAQAAIAAJ.

[29] A. Mersmann, Crystallization Technology Handbook, CRC Press, 2001, https://books.google.com.br/books?id=yRWa8zSjag4C.

[30] D. Elwell, H.J. Scheel, Crystal growth from high-temperature solutions, Academic Press, https://books.google.com.br/books?id=lDShpwAACAAJ, (1975).

[31] I.K. Bonev, K. Kouzmanov, Fluid inclusions in sphalerite as negative crystals: a case study, Eur. J. Mineral. 14 (2002) 607–620, https://doi.org/10.1127/0935-1221/2002/0014-0607.